

Kinetic and thermodynamic study of the separation of omeprazole enantiomers by HPLC using a polysaccharide carbamate as chiral stationary phase

Alessandra Ferraiolo de Freitas¹, Kátia Roberta Anacleto Belaz², Quezia Bezerra Cass²
and Cesar Costapinto Santana^{3,*}

¹Department of Biotechnological Processes, School of Chemical Engineering, State University of Campinas – UNICAMP, P.O. Box 6066, 13083 – 970 Campinas – SP, Brazil,

²Department of Chemistry, Federal University of São Carlos – UFSCar, P.O. Box 676, 13560 – 000 São Carlos – SP, Brazil, ³Department of Process Engineering, UNIT/NUESC, Av. Murilo Dantas 300, CEP 49032-490, Aracaju, SE, Brazil

ABSTRACT

Experimental results for the separation of R,S-omeprazole enantiomers obtained on preparative columns packed with amylose tris(3,5-dimethylphenylcarbamate) chiral stationary phase are presented. The total porosity was measured by using the non-retained compound 1,3,5-Tri-*tert*-butylbenzene. The efficiency of columns was characterized by the height equivalent to a theoretical plate (*HETP*) and a linear dependency has been found over tested flow rates. The *HETP* dependence on the mobile phase was determined to acquire the equilibrium and kinetics data of adsorption of racemic mixture of omeprazole. The retention factors and selectivity factors for the enantiomers of the omeprazole decreased with increasing temperature. The natural logarithms of the retention factors ($\ln k$) depended linearly on the inverse of temperature ($1/T$). van't Hoff plots afforded thermodynamic parameters, such as the apparent change in enthalpy (ΔH^0) and the apparent change in entropy (ΔS^0) for the transfer of analyte from the mobile to the stationary phase. Thermodynamic adsorption parameters (ΔH^0 and ΔS^0) were calculated in order to promote an understanding of the driving forces for retention

in this chromatographic system. Frontal analysis method was applied for the determination of the adsorption isotherms for the enantiomers of omeprazole. The isotherms, for both enantiomers, were adjusted satisfactorily to the Langmuir model.

KEYWORDS: adsorption isotherm, chiral stationary phase, enantiomer separation, hydrodynamic characterization, liquid chromatography, mass transfer, omeprazole, van't Hoff plot

INTRODUCTION

Due to the strict regulations of the US Food and Drug Administration and other regulatory institutions worldwide, the enantiomeric purity of chiral compounds used as intermediates or produced in the pharmaceutical industry has become a major concern. Nowadays, there is real interest in this industry in separation processes aiming at separating enantiomers by economically viable methods and to produce them at a high enantiomeric purity [1].

In the last decade, chiral chromatography has become a more and more important separation process for the purification of pharmaceuticals and other added-value products. One reason for the preference of chromatography is that the process allows both high yields and purity of

*cesarcsantana@gmail.com.br

both enantiomers. On the other hand, this technique is applicable to a wide variety of racemic mixtures, since chromatographic stationary phases for enantiomer separation are now available [2]. Batch chromatography is usually the preferred method when amounts from a few mg up to about 100 g of purified enantiomer are desired. When larger amounts are required, ranging from several hundred grams to kilograms, the simulated moving bed (SMB) is often a more efficient alternative [3].

In preparative chromatography, throughput is defined as the amount of purified material per unit of time and per unit of mass of stationary phase. Different factors affect throughput, namely, the loading capacity of the chiral stationary phases, column efficiency, selectivity, temperature, column size and feed flow rate. Also, feed concentration is a very important variable, which itself depends on the solubility of the solute [4].

Most of the chiral selectors are obtained from natural and synthetic sources. Derivatized amyloses and derivatized celluloses as chiral stationary phases have promising chiral recognition properties and high loading capacity. Both chiral stationary phases consist of tris(3,5-dimethylphenylcarbamate)-D-glucose units as chiral adsorbing sites and are offering a great versatility for separating a wide range of chiral compounds [5]. In all chromatographic modes, mainly the concentration and nature of the mobile phase components, together with additional variables, such as the flow-rate and the pH of the mobile phase, control the selectivity and retention factors. Significant effects can also be seen by altering the temperature [6, 7].

The variables, temperature and solute concentration usually affects resolution (R_s) and separation factor (α). Separation factor usually decreases as the temperature is increased. This occurs because the partition coefficients and therefore the free energy change (ΔG^0) of transfer of the analyte between the stationary phase and the mobile phase vary with temperature. This is the thermodynamic effect. In the case of multicomponent or ionizable mobile phases or an ionizable solute, both the distribution of the solvent components and the pK_a of the ionizable compound may vary with temperature.

Another completely different effect of temperature is the influence on viscosity and on diffusion

coefficients. This is largely a kinetic effect, which improves efficiency (i.e. peak width). There are two different mass transfer effects here. One is mobile phase mass transfer. An increase of temperature reduces the viscosity of the mobile phase. However an increase of temperature also increases the diffusion coefficient of the solute in both the mobile phase and the stationary phase, and it decreases the viscosity of the stationary phase (enhancing stationary phase mass transfer). Temperature increase often produces a trade-off on the resolution. The increased efficiency is good for resolution, while the decrease of the peak-to-peak separation decreases resolution. In highly efficient separations (regular achiral HPLC), there is usually little to be gained by increasing the temperature. In less efficient separations, however, where there is an adequate peak-to-peak distance as in many chiral separations, the gain in efficiency sometimes outweighs the loss in peak-to-peak separation when the temperature is increased. However, whether raising temperature is beneficial or not its effect must be determined on a case-by-case basis. Enantiomeric separations are carried out on chiral stationary phases (CSPs) that frequently have a relatively low saturation capacity. The CSPs are mostly composed of silica gel with only a few chiral elements that rapidly overload. Therefore, these separations are usually carried out under strongly nonlinear conditions [8, 9]. The determination of equilibrium isotherms is the prerequisite for the calculation of band profiles in all chromatographic processes, for the systematic investigation of the consequences on the production rate of changes made in the experimental conditions, and for the optimization of the design and operation of new separation methods. The adsorption isotherm represents all the possible interactions, attractive as well as repulsive, between the solute molecules and the stationary phase. With enantiomeric mixtures, the diastereomeric or enantioselective interactions are the only ones responsible for the separation [10].

The adsorption isotherms models relate the composition of the two phases at equilibrium. Linear models are valid only under the experimental conditions used in analytical chromatography, at low concentrations. To achieve economical productivity, preparative chromatography must be

conducted at high concentrations. Under such conditions, the isotherms are rarely linear. For mixtures, the amount of a compound adsorbed at equilibrium depends usually not only on its own concentration in the solution but also on the composition of the entire solution. In almost all known cases, isotherms are competitive, i.e. the amount of one compound adsorbed in equilibrium with a constant concentration of this compound decreases with increasing concentrations of the other feed components.

The objective of this work is to investigate hydrodynamic and sorption properties of the preparative column packed with amylose tris(3,5-dimethylphenylcarbamate) chiral adsorbent. Pulse experiments with diluted solutions were accomplished to obtain total porosity, Henry constants, axial dispersion and mass transfer coefficients and thermodynamic parameters. Experiments with concentrated solutions were carried out to obtain adsorption isotherms. These parameters will be employed to design the operating conditions in a continuous chromatographic SMB unit.

MATERIALS AND METHODS

Materials

The racemic mixture of omeprazole was supplied by Cristália Pharmaceutical Company (Itapira-São Paulo, Brazil). 1,3,5-Tri-*tert*-butylbenzene (TTBB) was purchased from Aldrich (USA). The HPLC-grade methanol used as mobile phase in this work, in which omeprazole is easily dissolved was obtained from J. T. Baker (USA).

Omeprazole, 5-methoxy-2-[[[4-methoxy-3,5-dimethyl-2-pyridinyl)methyl] sulphinyl]-1*H*-benzimidazole (Figure 1), a substituted benzimidazole compound and prototype anti-secretory agent, is the first of the "proton pump inhibitors" widely used for the prophylaxis and treatment of gastro-duodenal ulcers and for the treatment of symptomatic gastro-oesophageal reflux. It acts by interaction with H⁺/K⁺ ATPase in the secretory membranes of the parietal cells and is very effective in the treatment of Zollinger–Ellison syndrome.

Omeprazole contains a tricoordinated sulphur atom in a pyramidal structure and therefore can exist in two different optically active forms, R-(+)-

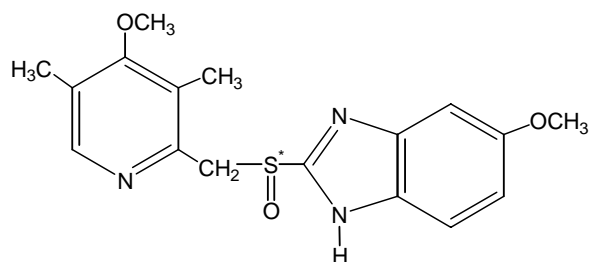


Figure 1. Chemical structure of omeprazole.

and S-(-)-omeprazole. Omeprazole was first approved as a racemic mixture, but the S-(-)-isomer was recently introduced on the market. Both enantiomers have a similar inhibitory effect on acid formation in isolated gastric glands from rabbits, but R-(+)-omeprazole is hydroxylated by cytochrome P450 CYP2C19 enzyme, resulting in an almost twofold increase in the plasma concentration for the S-(-)-isomer than for racemic omeprazole after the administration of equivalent doses [11].

Omeprazole enantiomers were separated using columns packed with amylose tris(3,5-dimethylphenylcarbamate) supported on a matrix of aminopropylated silica (Luna NH₂) with an average particle diameter of 10 μm and average pore diameter of 100 Å. The chiral stationary phase was prepared as reported by [12]. A semi-preparative column (250 mm x 1 mm I.D.) was packed with the prepared stationary phase under a pressure of 7500 psi. The average mass of chiral stationary phase in the column was 16.5 g.

Experimental procedure

Structure of the package, kinetic and thermodynamic parameters

The chromatographic system was conditioned by passing the eluent through the column until a stable baseline signal is obtained prior to every experiment. All chromatograms were obtained under isocratic conditions with methanol as a mobile phase. The mobile phase was previously degasified in a Cole Parmer 8892 ultrasonic bath. The hold-up volume was measured and corrected for the dead volume contribution of the liquid chromatography, by replacing the column with a zero-volume connector. Detection was carried out at 302 nm. A thermostatic bath controlled the

column temperature by circulating water through a plastic jacket in which the column was placed.

The total porosity as well as the bed porosity was determined by small chromatographic pulses (20 μL) of TTBB. The chromatographic peaks for non-retained tracer were obtained at flow rates from 1.0 mL/min to 4.0 mL/min.

The experiments for determination of equilibrium parameters for linear adsorption and mass transfer coefficients were accomplished at different mobile phase flow rates (1.0-4.0 mL/min) at 298 K. Momentum analysis was made with the experimental data resulted from small pulses (20 μL) of omeprazole enantiomers injected into the column after a time interval necessary to stabilize the system. Thermodynamic parameters were determined from response chromatographic peaks. An amount of 20 μL of dilute solutions were injected into the column at different temperatures (298, 303 and 323 K) at mobile phase flow rate of 1.0 mL/min.

Frontal analysis

The adsorption isotherm was measured using the frontal analysis method, which was performed in the conventional way using the available multichannel solvent delivery system. One pump was transferring the sample solution through the column until the outlet concentration had reached the inlet concentration; afterwards the second pump was used to deliver the solution of the mobile phase. Subsequently the whole system was re-equilibrated with pure mobile phase.

The experiments were carried out at a constant temperature of 298 K and at flow rate 2.0 mL/min. The breakthrough curves were measured in a concentration range between 1.0 and 4.0 mg/mL. Due to the limit of chromatographic system detection, the UV-vis detector signal was monitored at 350 nm. All the measurements were repeated two times and the isotherm data calculated by averaging the corresponding concentration data.

Each breakthrough curve gave one data point of the equilibrium isotherm. The adsorbed amount, q (mg/mL of adsorbent), of the solute in the stationary phase at equilibrium with a given concentration, C (mg/mL) can be calculated by a mass balance. The equilibrium data were fitted to Langmuir isotherm model.

Mathematical methods

Total porosity and bed porosity

Three different types of column porosity, which are total porosity (ε_T), bed porosity (ε), and the particle porosity (ε_p), are related by the equation [13].

$$\varepsilon_T = \varepsilon + (1 - \varepsilon)\varepsilon_p \quad (1)$$

The total porosity can be evaluated from the zero retention time of a non-retained component to the stationary phase. For a component that enters the pore system, but does not adsorb on the surface of the stationary phase, the retention time of such a component is given by Duan, Ching and Swarup [14].

$$t_0 = \frac{V_c \varepsilon_T}{V} = \frac{L \varepsilon_T}{u} \quad (2)$$

where V_c is the total column volume, L the column length, and u and \dot{v} are the superficial velocity and volumetric flow rate of mobile phase, respectively.

In order to evaluate the bed porosity, the following correlation was used in this work, which was suggested by Ruthven [15].

$$\varepsilon_T = 0.45 + 0.55\varepsilon \quad (3)$$

Moment analysis and plate height equation

The hydrodynamics of a chromatographic column can be described through the analysis of the residence-time distribution of the eluent, which is derived from the response curve. This response curve contains information associated with the properties of the column, which include the equilibrium and mass transfer parameters. The method of moment analysis is well-proved method to determine the hydrodynamics of the column.

By definition of the moments of a distribution, the n^{th} moment of the band profile at the exit of a chromatography bed of length $z = L$ is

$$M_n = \int_0^{\infty} C(t, L)^n dt \quad (4)$$

Due to greater physical significances, the first moment is normally defined as normalized moment

and moments higher than the first are defined as central moments, which are measured relative to the first moment:

$$\mu_1 = \frac{M_n}{M_0} = \frac{\int_0^{\infty} C(t, L) dt}{\int_0^{\infty} C(t, L) dt} \quad (5)$$

$$\bar{\mu}_2 = \sigma^2 = \frac{\int_0^{\infty} C(t, L) (t - \mu_1)^2 dt}{\int_0^{\infty} C(t, L) dt} \quad (6)$$

By definition, the zero moment of the concentration profile of an eluted peak is simply the area of the peak. The first moment is the center of gravity of the concentration profile. In chromatography, it relates to peak retention time and therefore to the strength of adsorption. It will coincide with the peak maximum only when the peak is symmetrical. The second moment is peak variance, which is chromatographically related to peak spreading, caused by departures from linear adsorption isotherms and by mass transfer resistances.

Thus, the first and second moments can be expressed as [16]:

$$\mu_1 = t_R = \frac{L}{u_*} \left[1 + \left(\frac{1-\varepsilon}{\varepsilon} \right) \varepsilon_p + \left(\frac{1-\varepsilon}{\varepsilon} \right) (1 - \varepsilon_p) H \right] = \frac{L}{u_*} \left[1 + \left(\frac{1-\varepsilon}{\varepsilon} \right) K \right] \quad (7)$$

$$\bar{\mu}_2 = \sigma^2 = \frac{2L}{u_*} \left\{ \frac{D_L}{u_*^2} \left[1 + \left(\frac{\varepsilon}{1-\varepsilon} \right) \frac{1}{K} \right]^2 + \left(\frac{\varepsilon}{1-\varepsilon} \right) \frac{1}{K k_m} \right\} \quad (8)$$

where u is the superficial velocity of the solvent through the bed, H the Henry constant, u_* the interstitial velocity ($u_* = u/\varepsilon$) of mobile phase and k_m the mass transfer coefficient.

From the moment analysis of the solution of the general rate model in the Laplace domain, we can obtain the expression for the height equivalent to a theoretical plate (*HETP*) which equals:

$$HETP = \frac{L}{N} = \frac{\sigma^2}{\mu^2} L = \frac{2D_L}{u} + 2u \left(\frac{\varepsilon}{1-\varepsilon} \right) \frac{1}{k_m K} \left[1 + \left(\frac{\varepsilon}{1-\varepsilon} \right) \frac{1}{K} \right]^{-2} \quad (9)$$

where

$$K = \varepsilon_p + (1 - \varepsilon_p) H \quad (10)$$

and

$$N = \frac{16d_R^2}{w_b^2} = 5,54 \left(\frac{d_R}{w_h} \right)^2 \quad (11)$$

Equation 9 contains two separate parameters of interests, the axial dispersion coefficient and the overall mass transfer coefficient. It is evident from the equation that the contributions of axial

dispersion and the various mass transfer resistances are linearly additive [13].

For a given separation, in which the system, packing and solute, are already defined, the *HETP* is a function of the mobile phase (u). One typical function is the van Deemter equation

$$HETP = A + \frac{B}{u} + Cu \quad (12)$$

The first two terms include the effects of molecular diffusion in the axial direction and axial dispersion, while the third term accounts for the

contributions from fluid film mass transfer, particle diffusion, and slow, sorption kinetics.

In a liquid system, the molecular diffusivities of the liquids are too small to contribute significantly to axial dispersion, even at low Reynolds numbers. Therefore, the molecular diffusivities in the systems studied can be neglected, leading to the linear form:

$$H = A + Cu \quad (13)$$

where

$$A = \gamma_2 d_p u \quad (14)$$

and

$$C = 2 \left(\frac{\varepsilon}{1-\varepsilon} \right) \frac{1}{Kk_m} \left[1 + \left(\frac{\varepsilon}{1-\varepsilon} \right) \frac{1}{K} \right]^{-2} \quad (15)$$

The differences between the various expressions reported in the literature for the dependence of the column *HETP* on the experimental parameters result from the use of different expressions for the axial dispersion D_L and mass transfer coefficient k_m .

Axial dispersion in packed beds

The sources of band broadening of kinetic origin include molecular diffusion, eddy diffusion, the mass transfer resistances and the finite rate of the kinetics of adsorption-desorption. Thus, it is important to study diffusion in porous media. The two main mechanisms contributing to axial dispersion are molecular diffusion and eddy diffusion. In a packed bed, it is impossible for the mobile phase to move very far along a straight line without hitting the surface of a particle. The channels follow tortuous paths around the particles. In a first approximation, molecular diffusion and eddy diffusion are additive, and the axial dispersion coefficient D_L , is given by

$$D_L = \gamma_1 D_m + \gamma_2 d_p u \quad (16)$$

where D_m is the molecular diffusivity, γ_1 and γ_2 are geometrical constants, whose values are usually around 0.7 and 0.5 respectively, and d_p is the particle diameter.

The second approximation was suggested by Chung and Wen [17]. It can be expressed as follows:

$$Pe = \frac{L}{\varepsilon d_p} \left[0,2 + 0,011 Re^{0,48} \right] \quad (17)$$

where $Re = (\gamma \varepsilon d_p u) / \eta$ is the Reynolds number, $Pe = uL / D_L$ is the column Peclet number and γ is the density of the mobile phase, and η is its viscosity. In this work, Equation 16 was used to evaluate the axial coefficients of the omeprazole enantiomers on chiral columns because of its simplicity.

Thermodynamic parameters

The enantiomer separation is based on the formation of reversible diastereoisomeric complexes, which are created by intermolecular interactions of enantiomers with the chiral selector [18]. These diastereoisomeric complexes must differ adequately in free energy for an enantiomer separation to be observed [19]. The formation process, for the R and S enantiomers can be characterized by thermodynamic parameters (ΔG^0 , ΔH^0 , ΔS^0).

In order to calculate thermodynamic parameters and to acquire information of value for an understanding of the enantiomeric retention, selectivity and mechanism on this CSP, van't Hoff plots must be constructed. The chromatographic retention, expressed by k , is related to the thermodynamic equilibrium constant (K) according to the following equation:

$$k = \phi K \quad (18)$$

in which ϕ is the phase ratio of the column ($\phi = 1 - \varepsilon/\varepsilon$). The free energy change for the process is expressed by [19]:

$$\Delta G^0 = \Delta H^0 - T\Delta S^0 = -RT \ln K = -RT \ln \left(\frac{k}{\phi} \right) \quad (19)$$

in which ΔG^0 is the standard free energy of transfer of the analyte from the mobile phase to the CSP, ΔH^0 is the enthalpy of transfer of the solute from the mobile phase to the CSP, ΔS^0 is the entropy of transfer of the solute from the mobile phase to the CSP, R is the gas constant, and T is the temperature.

Therefore, the dependence of chromatographic retention on temperature is described by the following equation [20].

$$\ln k = \frac{-\Delta H^0}{RT} + \frac{\Delta S^0}{R} + \ln \phi \quad (20)$$

This expression shows that a plot of $\ln k$ versus $1/T$ has a slope of $-\Delta H^0/R$ and an intercept of $-\Delta S^0/R + \ln \phi$ if ΔH^0 is invariant with temperature (i.e. a linear van't Hoff plot is obtained). This provides a convenient way of calculating the thermodynamic constants ΔH^0 and ΔS^0 for a chromatographic system if the phase ratio is known or can be calculated. Non-linear plots, however, often observed when the surface of stationary phase is heterogeneous and the retention

of a solute is influenced by mixed retention mechanism, or if there are conformational (or other) changes in the stationary phase with temperature [21].

The corresponding $\Delta(\Delta H^0)$ and $\Delta(\Delta S^0)$ values can be obtained as the differences $\Delta H_2^0 - \Delta H_1^0$ and $\Delta S_2^0 - \Delta S_1^0$, or can be estimated from the selectivity factor (α), which is related to the difference in Gibbs free energy of association for an enantiomeric pair $\Delta(\Delta G^0)$:

$$\Delta(\Delta G^0) = -RT \ln \alpha = \Delta(\Delta H^0) - T\Delta(\Delta S^0) = -RT \ln \alpha = -RT \ln \frac{k_2}{k_1} \quad (21)$$

If $\Delta(\Delta H^0)$ is constant within the temperature range, a straight line should be obtained when the natural logarithms of the α values of a given enantiomeric pair at different temperatures ($R \ln \alpha$) or $-\Delta(\Delta G^0)/T$ are plotted versus $1/T$. The slope is $-\Delta(\Delta H^0)$ and the intercept is $\Delta(\Delta S^0)$. The values of $\Delta(\Delta H^0)$ and $\Delta(\Delta S^0)$ obtained by the two different methods should be identical within experimental error.

The enantioselectivity expressed by Equation 21 through the property $\Delta(\Delta G^0)$, is mainly dominated by $\Delta(\Delta H^0)$ at relatively low temperatures. At higher temperatures, the entropic term $\Delta(\Delta S^0)$ increases and can reach the same value as the enthalpic term. At a given temperature named T_{iso} , a theoretical complete lack of chiral separation is obtained when $\Delta(\Delta G^0) = 0$. The predicted value of T_{iso} is therefore:

$$T_{iso} = \frac{\Delta(\Delta H^0)}{\Delta(\Delta S^0)} \quad (22)$$

At temperatures higher than T_{iso} , as calculated by Equation 22, the reverse elution order is observed. In general, T_{iso} is higher than the usual range of feasible temperatures for the great majority of enantiomers.

Adsorption isotherm

For the mathematical description of the chromatographic separation process the equilibrium

behavior of the species to be adsorbed is essential. There are different methods known for the measurements of adsorption isotherms [22, 23]. The most common methods are the frontal analysis (FA), the elution by characteristic point (ECP), the frontal analysis by characteristic point (FACP), and the perturbation method (PM) [9]. Frontal analysis is the most popular method, because of its high accuracy [24, 25].

The Langmuir isotherm is the most common model to describe nonlinear adsorption, although it is assumed to be a model too simple to account for the adsorption on chiral stationary phases. This model assumes that the adsorbent surface is homogeneous. It is convenient for many low energy surfaces as long as the interaction energy on each type of adsorption sites is low. In this case, the solute molecules rarely have to compete effectively with the solvent molecules adsorbed on the strongest sites. In a variety of cases, particularly among those encountered in enantiomeric separations, this restriction does not apply and a model that takes into account the heterogeneity of the adsorbent surface is needed [26] *The equation of the Langmuir model is given as:*

$$q_i = \frac{a_i c_i}{1 + b_i c_i} = \frac{b_i q_{s,i} c_i}{1 + b_i c_i} \quad (23)$$

where q_i is the concentration of component i adsorbed in the stationary phase; c_i , the concentration of component i in the mobile phase;

b_i , association equilibrium constant related to the energy of adsorption; $q_{s,i}$ ($= a_i/b_i$), the saturation capacity of the adsorbent and a_i ($= q_{s,i}b_i$) is the distribution coefficient (also called Henry constant).

Frontal analysis method

The frontal analysis method is also called the mass balance method [27]. In practice, it involves the frontal analysis of the solutes studied, e.g., two enantiomers, and a continuous monitoring of the column effluent by an on-line detector [28]. However, the main drawback concerning this method is the significant solute consumption and the long experimental time [29, 30, 31].

There are two main variants of this method, the staircase and the rectangular pulse methods. In the first case, demonstrated for competitive isotherms by [27], two solutions are mixed upstream the column and pumped through it at a constant flow rate. The first solution is the pure mobile phase. The second one is a solution of a mixture of the two compounds studied, dissolved in the mobile phase. The total concentration of these two compounds is increased stepwise, at appropriate times, and at constant relative composition of the mixture. Several sets of such data are successively acquired at different values of the relative composition.

The second method or rectangular pulse method is a variant of the first one. It consists of injecting a single step, washing the solution off the column with the pure mobile phase after the elution of the first step is completed, and starting again with a new, higher step. For a binary mixture of A and B, two plateaus are observed in the elution profiles. The first one is pure A (the less retained), the second one is composed of A and B, and their concentrations are the same as that of the sample injected. The main advantage of this method is that there is no need to analyze the composition of the intermediate plateau because only the pure first or lesser-retained component is eluted on this intermediate plateau.

The concentrations of A and B in the stationary phase can be given by the following expressions, component A (the less retained):

$$q_A = \frac{(V_2 - V_0)C_A - (V_2 - V_1)C_A}{V_a} \quad (24)$$

Component B (the more retained):

$$q_B = \frac{(V_2 - V_0)C_B}{V_a} \quad (25)$$

where q and C are the concentrations of i (A or B) in the stationary phase and in the mobile phase at equilibrium, respectively; C_A is the concentration of A on the intermediate plateau; V_1 and V_2 are the elution volumes of the two elution plateaus; V_D is the system hold-up volume (including the column hold-up volume, V_0 ($= V_T\varepsilon_T$)) and V_a ($= V_c(1 - \varepsilon_T)$) is the volume of the stationary phase in the column.

Since only the less retained component is obtained during the elution of the intermediate plateau, C_A is directly derived from the height of this plateau and no analysis of the effluent is required [31].

The main advantage of the rectangular pulse methods is that there is no need to analyze the composition of the intermediate plateau because only the pure first or lesser-retained component is eluted on this intermediate plateau. Accordingly, the instrumentation is simple and the measurements are faster and more accurate since they rely only on the determination of the concentration of the intermediate plateau and of the retention times of the two fronts [27].

RESULTS AND DISCUSSION

Hydrodynamic study of the chiral column

Chromatographic pulse experiments with non-retained compound were performed to determine the total porosity of the column. TTBB (Figure 2) has been widely used for the determination of the

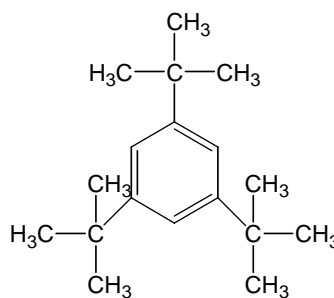


Figure 2. Chemical structure of TTBB.

column dead-time for amylose derivative chiral stationary columns [32]. Although the sorption of solutes for amylose derivatives is strongly supported by the phenyl group, the latter is shielded by the *tert*-butyl groups in TTBB. On the other hand, the molecular size of TTBB is relatively small (264.44 g/gmol).

According to Equation 7, t_R was plotted against L/u (Figure 3). The total porosity was determined from the slope of the straight line associated with Figure 3. The bed porosity was obtained from the correlation proposed by Ruthven [15] (Equation 3).

The values of ε_T and ε of column packed with amylose tris(3,5-dimethylphenylcarbamate) chiral stationary phase were found to be 0.680 and 0.418, respectively. The literature presents values of total porosity for Chiralpak AD commercial columns ranging from 0.610 up to 0.654 [1].

Elution profile of the omeprazole enantiomers and determination of linear equilibrium data

Figure 4 shows the elution profile of the omeprazole enantiomers. The less retained enantiomer is S-(-)-omeprazole and the more retained is R-(+)-omeprazole.

The system presented good performance separation. The separation factor (or selectivity)

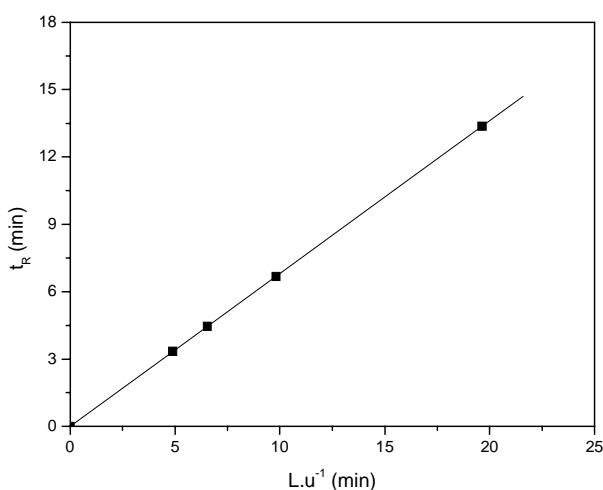


Figure 3. Plot of the first moment of TTBB versus the inverse of superficial velocity. Experimental conditions: TTBB concentration = 3.0 mg/mL; temperature = 298 K; mobile phase = methanol; injection volume = 20 μ L; flow rate = 1.0, 2.0, 3.0 and 4.0 mL/min; wavelength = 254 nm.

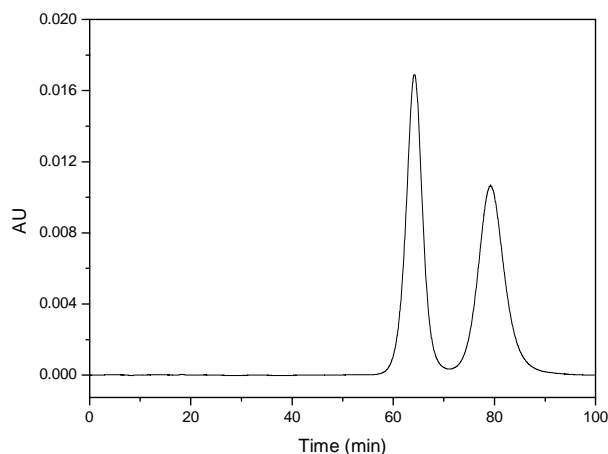


Figure 4. Elution profile of racemic mixture of omeprazole. Experimental conditions: racemic mixture concentration = 0.1 mg/mL; temperature = 298 K; mobile phase = methanol; injection volume = 20 μ L; flow rate = 1.0 mL/min; wavelength = 302 nm.

was found to be 1.29. In reference [33] the authors reported that in most separations with polysaccharide phases, complete separation of enantiomers is attained if selectivity is larger than 1.2. The retention and selectivity are mainly caused by polar carbamate residues, which, can interact with a solute via hydrogen bonding with NH and C=O groups, dipole-dipole interactions with C=O groups and π - π interactions [34, 35, 36, 37, 38, 39].

The retention times and width at half height of each peak provided important information for calculation of the equilibrium constants (Henry constants) and column efficiency in terms of theoretical plates.

The linear equilibrium constants for both enantiomers of omeprazole were determined experimentally using a similar procedure employed for the determination of the total porosity. In this case, from the slope of the straight lines obtained with the plots of t_R as a function of L/u , it was possible to calculate the values of K , using Equation 3. The reciprocal retention time of both pure enantiomers of R,S-omeprazole as a function of the flow rate is shown in Figure 5. The equilibrium constants were found to be 4.60 with $R^2 = 0.999$ for S-(-)-omeprazole and 6.32 with $R^2 = 0.999$ for R-(+)-omeprazole, respectively.

The results obtained under dilute conditions show that the K values are greater than unity. From these

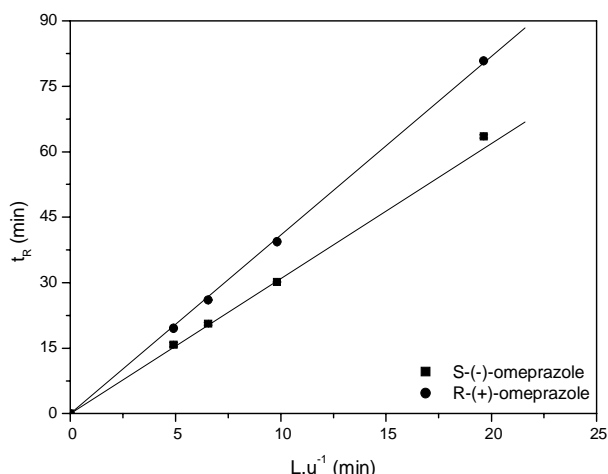


Figure 5. Plot of the first moment of omeprazole enantiomers versus the inverse of superficial velocity. Experimental conditions: racemic mixture concentration = 0.1 mg/mL; temperature = 298 K; mobile phase = methanol; injection volume = 20 μ L; flow rate = 1.0, 2.0, 3.0 and 4.0 mL/min; wavelength = 302 nm.

results we can conclude that a strong interaction occurs between the enantiomers and the chiral column. The chiral column presented a higher affinity for R-(+)-omeprazole than for S-(-)-omeprazole. This behavior can be attributed to different interactions that occur between the omeprazole enantiomers and the stationary phase [40].

The H was calculated from the retention times of a small pulse of racemic omeprazole according to Equation 10. The values were found to be 7.55 and 10.68 to S-(-)-omeprazole and R-(+)-omeprazole enantiomers, respectively.

Determination of the axial dispersion coefficients and mass transfer coefficient

The data from the first and second moments of both enantiomers and TTBB were utilized to assess the changes in column efficiency, according to Equation 9. The values of *HETP* were obtained by subtracting the contribution for the extra-column dispersion from the first and second moment. Plot of *HETP* versus *u* (Figure 6) of the omeprazole enantiomers were drawn, and according to Equation 9, the slope of the straight lines and the intersection furnished the overall mass transfer and the axial dispersion coefficients, respectively.

Figure 6 shows that the *HETP* presents a linear dependence of *u* with correlation coefficients $R^2 = 0.999$ for S-(-)-omeprazole and $R^2 = 0.999$ for R-(+)-omeprazole. In the tested range of flow rate (1.0-4.0 mL/min), the dependence of plate height upon the velocity was linear and the term of molecular diffusion has not been considered (minimum in the van Deemter plot). This result indicates that the effects of axial dispersion and mass transfer resistance control the efficiency of the column. The more-retained enantiomer presented a lower efficiency than less retained enantiomer.

Table 1 shows the axial dispersion and overall mass transfer coefficients, which were determined from the slope and the intercept of the linear relation between *HETP* and *u*.

Molecular diffusion contribution to *HETP* is considered approximately the same for all sorbates. This approximation is due to the method of determination for the axial mixing in a liquid system, which is made by the convective flow pattern built in the bed. This implies that all solutes should present the same *HETP*, at zero

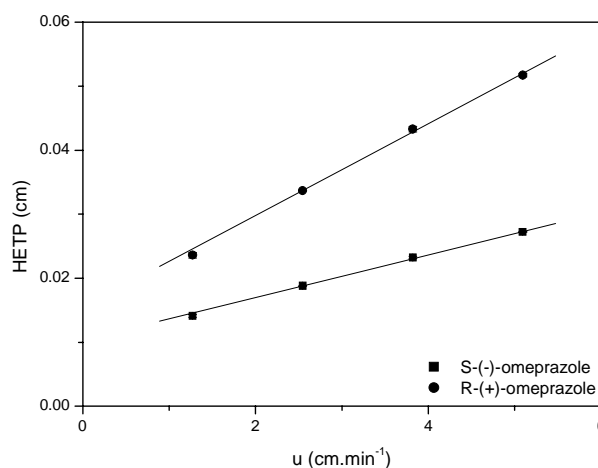


Figure 6. van Deemter plot for omeprazole enantiomers.

Table 1. Axial dispersion and overall mass transfer coefficients.

	S-(-)-omeprazole	R-(+)-omeprazole
D_L (cm ² .min ⁻¹)	$5.17 \pm 0.19 u$	$7.65 \pm 0.45 u$
k_m (min ⁻¹)	65.46 ± 1.32	26.61 ± 0.73

mobile phase superficial velocity. The difference among the values of the D_L can be due to experimental errors caused by particle of different size distribution [41].

According to the magnitude of the k_m values, a low mass transfer rate is observed in the column. The difference among the k_m values could be due to the difference in the kinetics of adsorption and desorption processes. The more retained enantiomer has the least mass transfer coefficient in the CSP compared with the less retained enantiomer. Similar results were obtained by [13, 14].

Thermodynamic parameters

The influence of the column temperature on the retention is summarized by the van't Hoff plot in Figure 7. In the present study, the plots of $\ln k$ versus $1/T$ can be fitted by straight lines, which shows the retention of the analyte decreasing as the column temperature increases. It may be said that with increasing temperature the analytes have smaller adsorption and the migration through the column is faster. The plot of the separation factor, α , versus absolute temperature is shown in Figure 8.

From the slope and the intercept of the van't Hoff plot, the enthalpy of transfer and the standard entropy of transfer were calculated, respectively.

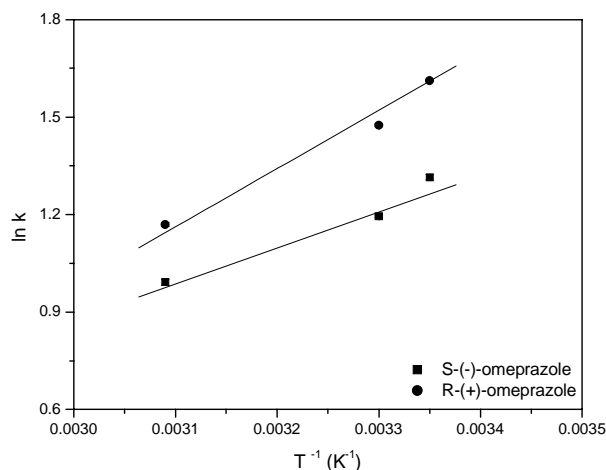


Figure 7. Dependence of natural logarithms of retention factors on the inverse temperature for R,S-omeprazole enantiomers. Experimental conditions: racemic mixture concentration = 0.1 mg/mL; temperature = 298, 303 and 323 K; mobile phase = methanol; injection volume = 20 μ L; flow rate = 1.0 mL/min; wavelength = 302 nm.

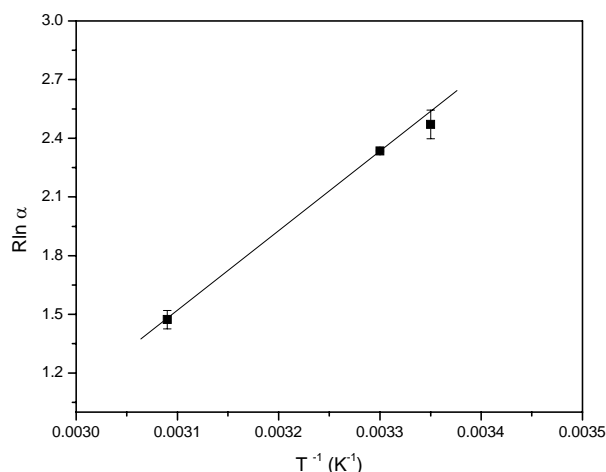


Figure 8. Plot of the separation factor of R,S-omeprazole enantiomers versus absolute temperature. Experimental conditions: racemic mixture concentration = 0.1 mg/mL; temperature = 298, 303 and 323 K; mobile phase = methanol; injection volume = 20 μ L; flow rate = 1.0 mL/min; wavelength = 302 nm.

The obtained thermodynamic parameters are reported in Table 2.

The ΔH^0 values calculated from the slopes of the plots by using Equation 20 are negative. This indicates that the transfer of the enantiomers from the mobile to the stationary phase is enthalpically favored. The enthalpy change for the second-eluted isomer is always greater (i.e. more negative) than that for the first-eluted isomer. This means that the association between the second-eluted enantiomer and the CSP is more favorable than for the first-eluted enantiomer.

As regard the ΔS^0 values, negative values were observed. The values for the first-eluted enantiomer were always more positive than those for the second-eluted enantiomer. The second-eluted enantiomer had more negative enthalpy and, at the same time, more negative entropy value. The two enantiomers (of a pair) must be solvated identically in mobile phase, but may release a different number of solvent molecules when they associate with the CSP. The contribution to ΔS^0 can be different for both enantiomers. Since the second-eluted enantiomers have more negative ΔS^0 values, they may have fewer degrees of freedom on the CSP (i.e. they held at more points or are less able to move or rotate or a smaller number

Table 2. Thermodynamic parameters of enantioseparation.

Compound	ΔS ($\text{J}\cdot\text{mol}^{-1}\text{K}^{-1}$)	ΔH ($\text{kJ}\cdot\text{mol}^{-1}$)	R^2	$\Delta\Delta S$ ($\text{J}\cdot\text{mol}^{-1}\text{K}^{-1}$)	$\Delta\Delta H$ ($\text{kJ}\cdot\text{mol}^{-1}$)	R^2
Q = 1.0 mL/min						
S-(-)-omeprazole	-24.26 ± 1.10	-9.20 ± 0.34	0.936	-11.09 ± 0.68	-4.07 ± 0.21	0.999
R-(+)-omeprazole	-40.48 ± 1.02	-14.90 ± 0.30	0.995			

of solvent molecules may be displaced by analyte when it associates with the CSP). Chiral recognition requires three or more points of simultaneous interactions between the CSP and the chiral analyte. This appears likely for the second-eluted enantiomer and somewhat less probable for the first-eluted enantiomer.

The more negative $\Delta(\Delta H^0)$ values mean that the interactions for these analytes are enthalpically favored.

The isoenantioselective temperature determined in this work (366.80 K) was higher than the working temperature range (298-323 K). It has been shown, that the (-)-enantiomer eluted prior to (+)-enantiomer. From the aforementioned data (Table 2), it has been concluded that the enantiomeric of omeprazole on the amylose tris(3,5-dimethylphenylcarbamate) chiral stationary phase is enthalpy driven.

Frontal chromatography experiments (or Adsorption isotherms)

Figure 9 shows the Scatchard plot, which was plotted with to determine if the isotherm model is homogeneous or heterogeneous. The Scatchard plot is linear and this indicates that the Langmuir model can be used to describe the adsorption isotherm [42, 43, 44].

Figure 10 shows the equilibrium isotherms obtained for the adsorption of the omeprazole enantiomers on amylose tris(3,5-dimethylphenylcarbamate) chiral stationary phase. The isotherms exhibit a significant deviation from linearity and the data obtained were correlated by Langmuir model. Values of the Langmuir model parameters are shown in Table 3. The non-linear fitting of the Origin 6.0 software package

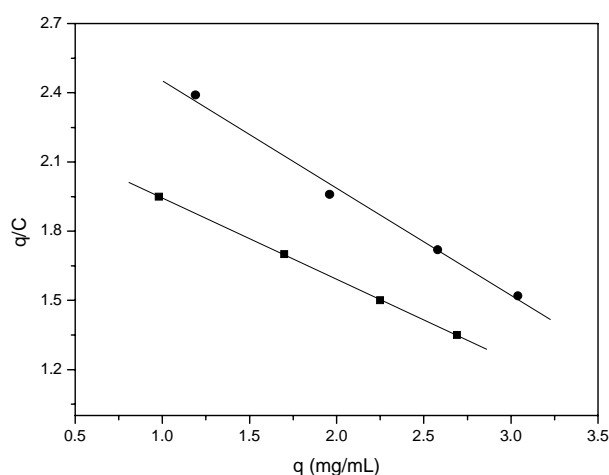


Figure 9. Scatchard plot from experimental data. The black squares were obtained for S-(-)-omeprazole while the black diamonds refers to R-(+)-omeprazole.

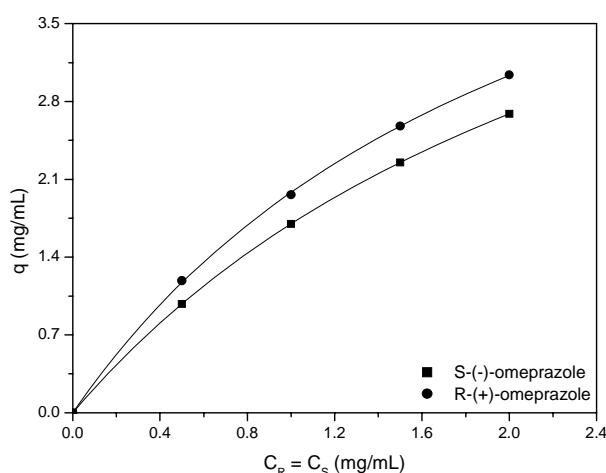


Figure 10. Adsorption isotherms of the R,S-omeprazole on the amylose tris(3,5-dimethylphenylcarbamate) chiral stationary phase at 298°C. Experimental conditions: racemic mixture concentration = 1.0, 2.0, 3.0 and 4.0 mg/mL; temperature = 298 K; mobile phase = methanol; flow rate = 2.0 mL/min; wavelength = 350 nm.

Table 3. Adsorption isotherm parameters determined by frontal analysis.

	<i>a</i>	<i>b</i> (L/g)	<i>q_s</i> (mg/mL)	<i>R</i> ²
S-(-)-omeprazole	2.310 ± 0.004	0.359 ± 0.002	6.433	0.999
R-(+)-omeprazole	2.856 ± 0.053	0.441 ± 0.020	6.475	0.999

(Microcal Software) was employed to obtain an estimate of these parameters. Each isotherm parameter in Table 3 is presented with its corresponding standard deviation estimate.

For the range of concentration investigated, it was possible to observe a considerable difference between the isotherms of each omeprazole enantiomers due to a higher adsorption capacity of CSP R-(+)-omeprazole (more retained enantiomer) than for S-(-)-omeprazole (less retained enantiomer). The simplicity and the good adjustment obtained by the Langmuir model indicate that this model would be preferred for the adjustment of our data.

CONCLUSION

Moment analysis allowed the determination of the overall mass transfer coefficient, axial dispersion coefficient, linear adsorption equilibrium constants, total and bed porosity of amylose tris(3,5-dimethylphenylcarbamate) column for the enantioseparation of omeprazole. The CSP exhibits a greater affinity for the R-(+)-omeprazole. The equilibrium constants are 4.60 and 6.32 for the S-(-) and R-(+)-enantiomers, respectively. The magnitude of the overall mass transfer coefficient shows that mass transfer on CSP column is very slow. We can conclude that the low mass transfer is due to the strong interaction between the enantiomers and the stationary phase. The axial dispersion coefficient was also estimated, and is approximately equal to 5.17 cm².s⁻¹ for S-(-)-omeprazole and 7.65 cm².s⁻¹ for R-(+)-omeprazole.

The effect of temperature on the retention of omeprazole was studied. In the temperature range under study (298-323 K), van't Hoff plots were linear. Changes in the enthalpies and entropies of solute transfer (mobile to stationary phase) were determined. Both the enantiomers exhibit negative enthalpy and entropy values. The more retained solute of the enantiomeric pair had the more negative ΔH^0 , indicating stronger interactions

with the CSP. The more retained enantiomer may form a stronger complex with CSP due to a greater number of points of interaction with the chiral surface. This could explain the negative value of ΔS^0 .

The method of frontal analysis was applied to quantify the adsorption equilibrium for the pure omeprazole enantiomers. The isotherms exhibit a deviation from linearity and the data obtained can be satisfactorily described by the Langmuir model.

The parameters obtained in this work will be useful for the design of operational conditions of the simulated moving bed (SMB) continuous chromatographic processes under linear conditions. The results from frontal analysis concerning the non-linear isotherms will be used for the design and operation of an SMB unit working under non-linear conditions.

ACKNOWLEDGMENTS

The authors are grateful to CNPq – BRAZIL for financial support and to the pharmaceutical company Cristália, for kindly providing the racemic omeprazole.

NOMENCLATURE

<i>A, B</i> and <i>C</i>	Coefficients of the Equation 12
<i>a_i</i>	Distribution coefficient
<i>b_i</i>	Association equilibrium Constant
<i>C_i</i>	Concentration of component <i>i</i> (A or B) in the mobile phase (mg.mL ⁻¹)
ΔG^0	Gibbs free energy (J.mol ⁻¹)
ΔH^0	Enthalpy (J.mol ⁻¹)
ΔS^0	Entropy (J.mol ⁻¹ .K ⁻¹)
<i>d_p</i>	Particle diameter (μm)
<i>D_L</i>	Axial dispersion coefficient (cm ² .s ⁻¹)
<i>D_m</i>	Molecular diffusivity (cm ² .s ⁻¹)
<i>HETP</i>	Height equivalent to a theoretical plate (cm)
<i>H</i>	Henry constant
<i>k</i>	Retention factor

k_m	Overall mass transfer coefficient (min^{-1})
K	Thermodynamic equilibrium constant
L	Column length (cm)
N	Plate number
Pe	Peclet number
q_i	Concentration of component i adsorbed in the stationary phase (mg.mL^{-1})
$q_{s,i}$	Saturation capacity of the adsorbent (mg.mL^{-1})
R	Gas constant ($\text{atm.L.mol}^{-1}.\text{K}^{-1}$)
Re	Reynolds number
t_0	Retention time of a non-retained component (min)
t_R	Retention time of the solute (min)
T	Temperature (K)
T_{iso}	Isoenantioselective temperature (K)
u	Superficial velocity of the solute (cm.s^{-1})
u_*	Interstitial velocity of mobile phase (cm.s^{-1})
V_0	Column hold-up volume (mL)
V_a	Adsorbent volume (mL)
V_C	Total column volume (mL)
V_D	System hold-up volume (mL)
\dot{V}	Volumetric flow rate of mobile phase (mL.min^{-1})
V_1	Elution volume of the first plateau (mL)
V_2	Elution volume of the second plateau (mL)

GREEK SYMBOLS

α	Separation factor (or selectivity)
φ	Phase ratio
μ	First moment (min)
μ_2	Second moment (min^2)
σ^2	Variance
ε_T	Total column porosity
ε	Bed porosity
ε_p	Particle porosity
η	Viscosity (cP)
λ	Wavelength (nm)
γ	Density of the mobile phase (g.mL^{-1})
γ_1 and γ_2	Geometrical constants

REFERENCES

- Mihlbachler, K., De Jesus, M. A., Kaczmarek, K., Sepaniak, M. J., Seidel-Morgenstern, A. and Guiochon, G. 2006, *J. of Chromatogr. A*, 1113, 148.
- Ribeiro, A. E., Graça, N. S. A., Pais, L. S. and Rodrigues, A. E. 2008, *Sep. Purif. Technol.*, 61, 375.
- Nicoud, R., Fuchs, M. G., Adam, P., Bailly, P. M., Küsters, E., Antia, F. D., Reuille, R. and Schmid, E. 1993, *Chirality*, 5(4), 267.
- Zabka, M. and Rodrigues, A. E. 2007, *Separ. Sci. Technol.*, 426, 739.
- Yashima, E. 2001, *J. of Chromatogr. A*, 906, 105.
- Péter, A., Torok, G., Armstrong, D. W., Toth, G. and Tourwe, D. 1998, *J. of Chromatogr. A*, 828, 177.
- Péter, A., Vékes, E. and Armstrong, D. W. 2002, *J. of Chromatogr. A*, 958, 89.
- Araújo, J. M. M., Rodrigues, R. C. R. and Mota, J. P. B. 2008, *J. of Chromatogr. A*, 1189, 302.
- Guiochon, G., Shirazi, S. G. and Katti, A. M. 1994, *Fundamentals of Preparative and Nonlinear Chromatography*, Academic Press, Boston.
- Cavazzini, A., Kaczmarek, K., Szabelski, P., Zhou, D., Liu, X. and Guiochon, G. 2001 *Anal. Chem.*, 73, 5704.
- Hassan-Alin, M., Andersson, T., Niazi, M. and Röhss, K. 2005, *Eur. J. Clin. Pharmacol.*, 60, 779.
- Matlin, S. A., Tiritan, M. E., Crawford, A. J., Cass, Q. B. and Boyd, D. R. 1994, *Chirality*, 6(2), 135.
- Wang, X. and Ching, C. B. 2002, *Separ. Sci. and Technol.*, 37(11), 2567.
- Duan, G., Ching, A. B. and Swarup, S. 1998, *Chem. Eng. J.*, 69, 111.
- Ruthven, D. M. 1984, *Principles of Adsorption and Adsorption Process*, John Wiley & Sons, New York.
- Arnold, F. H., Blanch, H. W. and Wilke, C.R. J. 1985 *J. of Chromatogr.*, 330, 159.
- Chung, S. F. and Wen, C. Y. 1968, *AIChE J.*, 14, 857.
- Rojkovičová, T., Lehotay, J., Krupčík, J., Fedurcová, A., Čižmárik, J. and Armstrong, D. W. 2004, *J. of Liquid Chrom. & Rel. Tech.*, 27(11), 1653.
- Cabusas, M. H. Y. 1998, PhD Thesis Virginia Polytechnic Institute and State University, Blacksburg.

20. Weng, W., Zeng, Q., Yao, B., Wang, Q. and Li, S. 2005, *Chromatographia*, 61(11/12), 561.
21. Fornstedt, T., Götmar, G., Andersson, M. and Guiochon, G. J. 1999, *J. Am. Chem. Soc.*, 121, 1164.
22. Kostova, A. and Bart, H. J. 2007, *Separ. Sci. Technol.*, 54, 340.
23. Seidel-Morgenstern, A. and Guiochon, G. 1998, *J. of Chromatogr. A*, 631, 37.
24. Felinger, A., Zhou, D. and Guiochon, G. 2003, *J. of Chromatogr. A*, 1005, 35.
25. Mihlbachler, K., Kaczmarski, K., Seidel-Morgenstern, A. and Guiochon, G. 2002, *J. of Chromatogr. A*, 955, 35.
26. Zhou, D., Cherrak, D. E., Kaczmarski, K., Cavazzini, A. and Guiochon, G. 2003, *Chem. Eng. Sci.*, 58, 3257.
27. Jacobson, J. M., Frenz, J. H. and Horváth, C. 1987, *Ind. Eng. Chem. Res.*, 26, 43.
28. Burger, D., Neumfiller, R., Yang, G. L., Engelhardt, H., Quiñones, I. and Guiochon, G. 2000 *Chromatographia*, 51(9/10), 517.
29. Arnell, R., Forssén, P. and Fornstedt, T. 2005, *J. of Chromatogr. A*, 1099, 167.
30. Kaczmarski, K. 2007, *J. of Chromatogr. A*, 1176, 57.
31. Sun, S., Yang, G., Sun, H., Wang, D. and Liu, H. 2001, *J. of Chromatogr. A*, 918, 13.
32. Guiochon, G. 2002, *J. of Chromatogr. A*, 965, 129.
33. Okamoto, Y. and Kaida, Y. 1994, *J. of Chromatogr. A*, 666, 403.
34. Chankvetadze, B., Yashima, E. and Okamoto, Y. 1995, *J. of Chromatogr. A*, 694, 101.
35. Okamoto, Y. and Kaida, Y. 1990, *J. Res. Chromatogr.*, 13, 708.
36. Yashima, E. and Okamoto, Y. 1995, *B. Chem. Soc. Jap.*, 68, 3289.
37. Okamoto, Y., Kawashima, M. and Hatada, K. 1986, *J. of Chromatogr.*, 363, 173.
38. Zdzislaw, C. 1999, *Chirality*, 11(10), 790.
39. Zhao, Y. and Pritts, W. 2007, *J. of Chromatogr. A*, 1156, 228.
40. Silva, I. J. Jr., Veredas, V., Carpes, M. J. S. and Santana, C. C. 2005, *Adsorption*, 11, 123.
41. Jacobson, C. S., Seidel-Morgenstern, A. and Guiochon, G. 1993, *J. of Chromatogr. A*, 637, 13.
42. Cherrak, D. E., Khattabi, S. and Guiochon, G. 2000, *J. of Chromatogr. A*, 877, 109.
43. Gritti, F. and Guiochon, G. 2005, *J. of Chromatogr. A*, 1099, 1.
44. Samuelsson, J., Sajonz, P. and Fornstedt, T. 2008, *J. of Chromatogr. A*, 1189, 19.